

# Investigation of III-Nitride Materials for Space-Based Solar Cells

Abdelhak Bensaoula, Chris Boney

**Abstract—**Researchers are investigating the suitability of the material *InGaN* as a candidate for photovoltaic space power generation. The effect of growth parameters on the properties of the films is under study. Modeling of single junction *In<sub>x</sub>Ga<sub>1-x</sub>N* solar cell properties has been performed for  $x < 0.50$ .

**T**HERE IS AN INCREASING NEED for enhancing the power generation capacity in NASA space systems for long-term and complex missions like the International Space Station. For these applications, specific power (W/kg), power stowed volume (W/m<sup>3</sup>), and lifetime are of critical importance. It is well known that the theoretical efficiency of an ideal single junction solar cell is around 31%, with real-world achievable values closer to 26%. To achieve higher efficiencies, multiple layers with optimally chosen bandgap materials are required so that the device is sensitive to a larger fraction of the solar spectrum. Current technologies combine different material systems, such as the Group III-V and Group IV, into multiple junction (MJ) cells. Typically, the physical properties of different material families can be radically different, causing issues in device fabrication, performance, and lifetime.



Dr. Abdelhak Bensaoula

There is one emerging material family that has the capability of covering almost all of the usable solar emission range (0.5 - 3.0 eV) and that is the Group III-Nitrides, specifically the alloy *InGaN*. Based on the film composition, *InGaN* can cover a wide bandgap range from 0.70 eV up to 3.4 eV which would be ideal for high efficiency solar cell applications. In addition, it has recently been determined that the Nitride materials can offer exceptional radiation tolerance that is well beyond what can be achieved with conventional solar cell materials currently flown into space.<sup>1</sup> However, the Nitride materials are currently a much less mature technology than other III-V semiconductors and, therefore, will not likely have as high efficiency as their III-V counterparts. At the same time, however, they will degrade far less over the life of the mission. Therefore, a 32% efficient Nitride solar cell with no degradation will be equivalent, if not superior, to a III-V cell which would start at 36% efficiency but degrades to 30% at end-of-life (EOL).

The goal of this ongoing project is to determine the feasibility of the *InGaN* material system for use in high efficiency single and multijunction solar cells. Simulations of single junction *InGaN* solar cells were undertaken to predict the effect of structural defects on the performance of the devices. In order for *InGaN* to be a viable candidate, the layers must be of high structural quality with background doping levels in the low 10<sup>17</sup> cm<sup>-3</sup> range. A series of *InGaN* layers was fabricated under different growth conditions to reduce the background doping levels.

## Methodology

Simulations of *InGaN* films in photovoltaic structures were performed using in-house code written for Matlab (MathWorks Inc.). The calculations involved simulating the response of a *InGaN* p-i-n device over an AM0 spectral range of 0 - 4 eV. In simulations, many of the material parameters of *InGaN* were estimated based on interpolation between parameters for *GaN* and *InN*, most of which are present in the literature. However, some parameters are not yet known, especially for *InN*, and, in those cases, values from materials were assumed. For interpolation, either a linear or quadratic approximation based on the alloy composition was used.

We have used radio frequency Molecular Beam Epitaxy (MBE) to fabricate *In<sub>x</sub>Ga<sub>1-x</sub>N* films under different growth conditions. Important parameters included the substrate temperature, *In/Ga* ratio, total III/*N* ratio, and film growth rate. Photoluminescence has been used to estimate the bandgap of the *InGaN* layers, while capacitance-voltage measurements were used to determine the change in free carrier concentration as a function of growth conditions.

## Equipment

The growth equipment employed in our investigations of III-*N* materials is a custom-made molecular beam epitaxy chamber. The sample holder is compatible with substrates up to 2" in diameter and operates at temperatures as high as 900°C. Standard effusion cells are used for Group III and dopant flux delivery, which currently includes *Ga*, *Al*, *In*, *Si*, and *Mg*. Nitrogen atoms are generated by an EPI Uni-Bulb radio-fre-

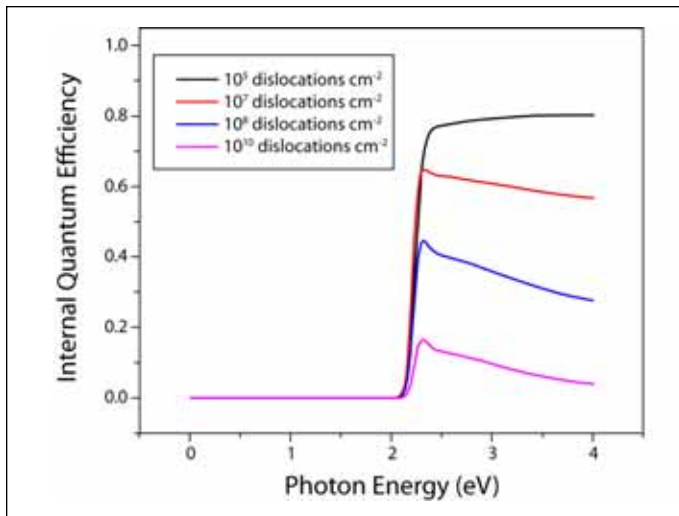


**Figure 1.** Calculation of the internal quantum efficiency of an  $In_{0.3}Ga_{0.7}N$  device under illumination by an AM0 spectra from 0 - 4 eV. The aerial defect density present in the layer has a profound effect on overall efficiency.

quency (RF) plasma source. *In-situ* characterization of the growth is carried out by reflection high-energy electron diffraction (RHEED). The chamber is pumped with a turbomolecular pump with a pumping speed of 2200 L/s resulting in a base pressure of  $5 \times 10^{-10}$  torr.

Photoluminescence measurements were excited by the 325 nm emission from a Melles Griot Series 56 *HeCd* laser, the resulting luminescence was dispersed by a 0.32 m focal length Jobin Yvon-Spex Triax320 monochromator and detected by a Hamamatsu R928 photomultiplier tube. Capacitance-voltage measurements were made using a Keithley Model 82 C-V system.

### Results and Discussion

Our simulations have verified that a reasonable structural quality is necessary for *InGaN* to be a candidate for solar cell applications. Figure 1 illustrates the strong effect that dislocation density has on the overall efficiency of a photovoltaic structure. The internal quantum efficiency as a function of the solar flux available above the earth's atmosphere (AM0 spectra from 0 - 4 eV) of an  $In_{0.3}Ga_{0.7}N$  (bandgap = 1.69 eV) structure is plotted for dislocation densities between  $10^5$   $cm^{-2}$  and  $10^{10}$   $cm^{-2}$ . The dramatic drop in efficiency stems from the scattering of the carriers in the film and results in a lowered minority carrier lifetime and, hence, lower diffusion length. Carriers generated in the depths of the structure can not successfully transport to the contacts of the device before re-combining and, thus, do not contribute to the photocurrent. At densities below approximately  $10^6$   $cm^{-2}$ , the dislocations do not have any effect because the distance between dislocations has become longer than the estimated intrinsic diffusion length in the  $In_{0.3}Ga_{0.7}N$  film. The overall internal quantum efficiency of the structure for each dislocation density is proportional to the area under the respective curves in Fig. 1. For  $10^7$   $cm^{-2}$ , the total efficiency has dropped by 22% relative to  $10^5$   $cm^{-2}$ , while for  $10^8$   $cm^{-2}$ , the total efficiency has

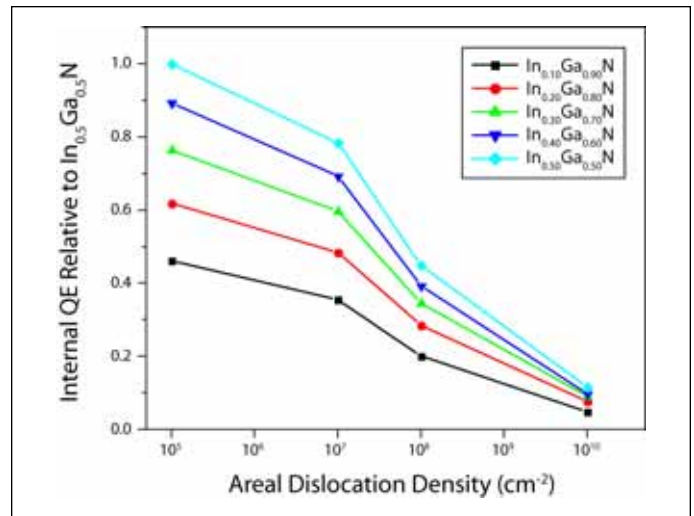


**Figure 2.** Calculation of the internal quantum efficiency for different compositions of *InGaN* photovoltaics under illumination by an AM0 spectra from 0 - 4 eV. The QE for the  $In_{0.5}Ga_{0.5}N$  was chosen as the maximum scale for the other compositions.

dropped to 55%; for  $10^{10}$   $cm^{-2}$ , total efficiency drops to 88%.

Similar simulations for  $In_xGa_{1-x}N$  compositions ranging between  $0.1 \leq x \leq 0.5$  have been performed to predict the efficiency as the bandgap of the material changes. As expected, the smaller bandgap materials (higher “ $x$ ”) have better efficiencies due to the wider spectral response they provide. Changes in the intrinsic material parameters as a function of “ $x$ ”, such as the effective mass of the carriers and the absorption coefficient near the bandgap, change the shape of the response curve slightly but do not have a strong effect on the final efficiencies. All compositions are essentially equally affected by the presence of a large number of dislocations. A graph summarizing the efficiencies of several  $In_xGa_{1-x}N$  compositions for different dislocation densities is shown in Fig. 2. The values for the internal quantum efficiency have all been scaled relative to the material with the highest efficiency ( $In_{0.5}Ga_{0.5}N$ ) that was simulated. A maximum of  $x = 0.5$  was chosen based on our belief that this composition represents an upper limit in terms of being able to achieve a film of both reasonable structural and electrical properties using current growth techniques.

Growth of  $In_xGa_{1-x}N$  films by MBE under different growth conditions—such as *In/Ga* ratio, total III/*N* ratio, and film growth rate—have been performed. To date, we have realized a maximum indium mole fraction of approximately 42% for single phase *InGaN*. Room temperature photoluminescence depicting this range of materials is shown in Fig. 3. The results of the bandgap based on the photoluminescence emission energy do not agree well with x-ray diffraction analysis of the film composition for high indium mole fractions. This is illustrated in Fig. 4. Capacitance-voltage measurements of the films reveal that the layers continue to have a high background *n*-type carrier concentration despite our modifications to the growth process. The high number of carriers is likely causing band-filling in the conduction band, which is altering the photolumines-

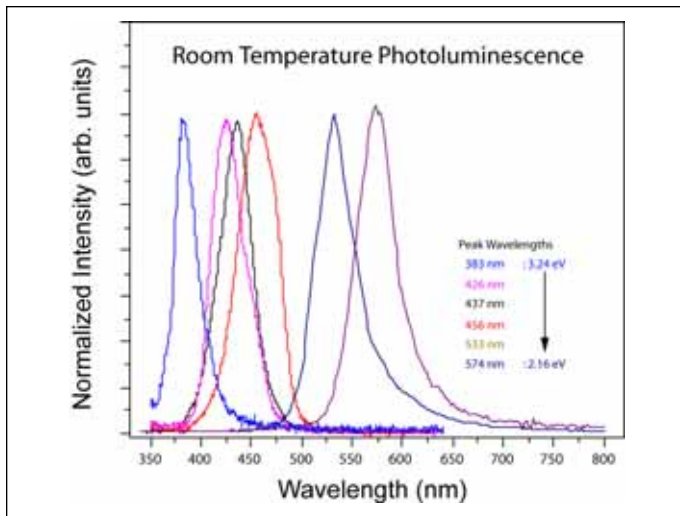


Figure 3. Photoluminescence of  $In_xGa_{1-x}N$  over the compositional range from  $0 < x < 0.42$ . The intensity of the luminescence has been normalized to highlight the shift of the emission peak.

cence transition energies to values higher than the actual bandgap of the  $InGaN$ . The excess carriers can not be accounted for by defects within the layers or by the contributions from the controllable growth conditions. We therefore conclude that we have an unknown variable in our fabrication process, and experiments are underway to determine its identity.

### Conclusions

$InGaN$  remains a potential candidate for space-based solar cells. Improvement in the optical and electrical properties of our layers is continuing. We have performed modeling of single junction  $InGaN$  solar cells to determine the effects of structural defects on device performance. As expected, large numbers of defects dramatically reduce the efficiency of solar cell devices. However, at defect levels below approximately  $10^6 \text{ cm}^{-2}$ , the efficiency is no longer affected. The fact that  $GaN$  templates for  $InGaN$  film growth are now becoming commercially available with defect densities below  $5 \times 10^7 \text{ cm}^{-2}$  means that the ultimate efficiency of  $InGaN$  photovoltaics will soon not be constrained by structural issues.

### References

<sup>1</sup>J. W. Ager III, J. Wu, K. M. Yu, R. E. Jones, S. X. Li, W. Walukiewicz, E. E. Haller, H. Lu, and W. J. Schaff, "Group III-Nitride Alloys as Photovoltaic Materials," *Proc., SPIE* 5530 (2004): 308-15.

### Publications

Starikov, D., C. Boney, R. Pillai, and A. Bensaoula. "Solar-Blind Dual-Band UV/IR Photodetectors Integrated on a Single Chip," *J. Experimental Nanoscience*. (In preparation.)

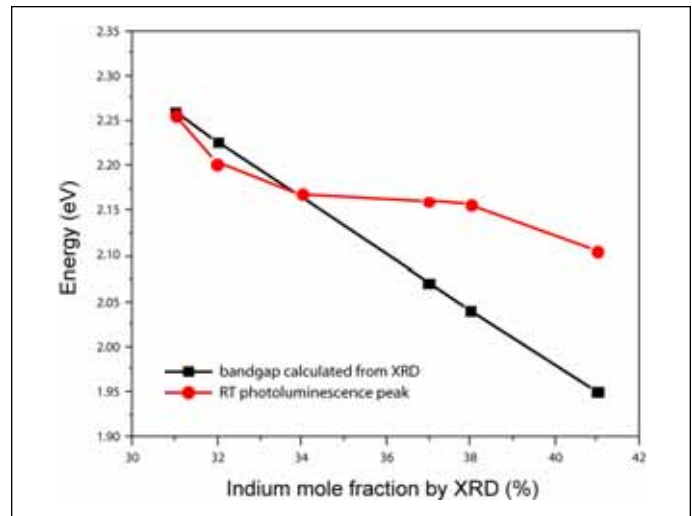


Figure 4. Discrepancy in the bandgap of  $In_xGa_{1-x}N$  as determined by x-ray diffraction and photoluminescence for values of  $x \geq 34\%$ . The photoluminescence is likely affected by band-filling effects due to the high carrier concentration in the films. This results in transition energies well above the actual bandgap of the material.

### Presentations

Starikov, D., A. H. Bensaoula, and A. Bensaoula. "High-Temperature Multi-Band Optical Sensors for Early Fire and Hazardous Object Detection," TEFT Proposal Presentation, Houston Technology Center, Oct. 10, 2005.

Starikov, D., C. Joseph, M. Boukadoum, and A. Bensaoula. "Chip-Based Integrated Filterless Multi-Wavelength Optoelectronic Bio-Chemical Sensors," Sensors for Industry Conf., Houston, TX, Feb. 8–10, 2005.

Starikov, D., N. Medelci, R. Pillai, A. Bensaoula, C. Joseph, and Z. Mouffak. "III Nitride-Based Optical Sensors Integrated with a TOF Mass Spectrometer for Aerosol Characterization," 51st AVS Intl Symposium, Anaheim, CA, Nov. 14–19, 2004.

### Funding and Proposals

"High-Stability III Nitride Based Stellar Simulator Optical Sources for In-Flight Calibration in a Super Wide Range of the Spectrum," NASA NRA ASTID-05, (CAM/IMS), 2006–2009, \$875,530. (Pending.)

"Integrated Broad-Band Optical Calibration Sources for Star Simulation," NSF Phase I SBIR project (IMS/CAM), 2006, \$100,000.

"Solid-State High Temperature Jet Engine Fire Detector," DoD (Air Force) Phase I and Phase II SBIR projects (IMS/CAM), 2004–2007, \$850,000.